MARTIN MARIETTA ENERGY SYSTEMS LIBRARIES

3 4456 0381132 9

ORNL/TM-12721

ornl

OAK RIDGE
NATIONAL
LABORATORY

MARTIN MARIETTA

Numerical Solution of a Tunneling Equation

C. Y. Wang
M. D. Chester
D. B. Batchelor
E. F. Jaeger

OAK RIDGE NATIONAL LABORATORY
CENTRAL RESEARCH LIBRARY
CIRCULATION SECTION
4500N ROOM 175
LIBRARY LOAN COPY
DO NOT TRANSFER TO ANOTHER PERSON
If you wish someone else to see this report, send in name with report and the library will arrange a loan.
UCN-7969 (3 9-77)

MANAGED BY
MARTIN MARIETTA ENERGY SYSTEMS, INC.
FOR THE UNITED STATES
DEPARTMENT OF ENERGY

This report has been reproduced directly from the best available copy.

Available to DOE and DOE contractors from the Office of Scientific and Technical Information, P.O. Box 62, Oak Ridge, TN 37831; prices available from (615) 576-8401, FTS 626-8401.

Available to the public from the National Technical Information Service, U.S. Department of Commerce, 5285 Port Royal Rd., Springfield, VA 22161.

This report was prepared as an account of work sponsored by an agency of the United States Government. Neither the United States Government nor any agency thereof, nor any of their employees, makes any warranty, express or implied, or assumes any legal liability or responsibility for the accuracy, completeness, or usefulness of any information, apparatus, product, or process disclosed, or represents that its use would not infringe privately owned rights. Reference herein to any specific commercial product, process, or service by trade name, trademark, manufacturer, or otherwise, does not necessarily constitute or imply its endorsement, recommendation, or favoring by the United States Government or any agency thereof. The views and opinions of authors expressed herein do not necessarily state or reflect those of the United States Government or any agency thereof.

ORNL/TM-12721
Dist. Category UC-427

Fusion Energy Division

Numerical solution of a tunneling equation

C. Y. Wang
M. D. Carter
D. B. Batchelor
E. F. Jaeger

DATE PUBLISHED — April 1994

Prepared for the
Office of Fusion Energy
Budget Activity AT 05 20 21 0

Prepared by
OAK RIDGE NATIONAL LABORATORY
Oak Ridge, Tennessee 37831-6285
managed by
MARTIN MARIETTA ENERGY SYSTEMS, INC.
for the
U.S. DEPARTMENT OF ENERGY
under contract DE-AC05-84OR21400

MARTIN MARIETTA ENERGY SYSTEMS LIBRARIES

3 4456 0381132 9

CONTENTS

ABSTRACT v

1 INTRODUCTION 1

2 NUMERICAL METHOD 3
- 2.1 Fast wave incident from $-\infty$ 4
- 2.2 Fast wave incident from $+\infty$ 5
- 2.3 Slow wave incident from $+\infty$ 5

3 NUMERICAL SOLUTION 7
- 3.1 Fast wave incident from $-\infty$ 7
- 3.2 Fast wave incident from $+\infty$ 8
- 3.3 Slow wave incident from $+\infty$ 8

4 CONCLUSION 10

REFERENCES 11

ABSTRACT

A numerical method is presented to solve mode conversion equations resulting from the use of radio frequency (rf) waves to heat plasmas. The solutions of the mode conversion equations contain exponentially growing modes, and ordinary numerical techniques give large errors. To avoid the unphysical growing modes, a set of boundary conditions are found, that eliminate the unphysical modes. The mode conversion equations are then solved with the boundary conditions as a standard two-point boundary value problem. A tunneling equation (one of the mode conversion equations without power absorption) is solved as a specific example of this numerical technique although the technique itself is very general and can be easily applied to solve any mode conversion equation. The results from our numerical calculation agree very well with those found from asymptotic analysis.

1 INTRODUCTION

In radio frequency (rf) heating of fusion plasmas, the mode conversion from an incident fast wave to ion Berstein wave (IBW) plays an important role. The mode conversion process can be described by a fourth- or higher-order ordinary differential equation, which is called a mode conversion equation. Mode conversion equations can be solved globally by using multiple layer[1,2], finite difference[3], and finite element methods[4], or can be solved locally by using Green's function[5], shooting[6,7], mode expansion[8], and invariant imbedding methods[9]. In this paper we discuss only the numerical methods to solve the mode conversion equations locally. Mode conversion equations are very difficult to solve numerically because of exponentially growing components[10]. The idea of the Green's function method is to find a solution for simplified homogeneous equations and use it to construct integral equations.[5,11] The success of this technique depends on the numerical solutions of the homogenous equations, which are nontrivial and contain exponentially growing components too. The shooting method uses an initial value ordinary differential equation (ODE) solver to integrate mode conversion equations many times to find all independent solutions, from which transfer matrices are constructed.[7,10] A key to the success of this method is to avoid the effects from the exponentially growing components. This is done by calculating the transfer matrices at each step and stopping when the change of the parameters is small enough. If one integrates too far, the growing components will dominate the solutions and undermine the accuracy of the method. Although meaningful numerical results can be found by using this method, the method intrinsically is numerically unstable. The mode expansion method used in Ref. [8] has some arbitrariness on the effect of the exponentially growing modes, which is controlled by an input parameter. The invariant imbedding method isolates the exponentially growing mode from the other well-behaved solutions to the mode conversion equation and uses an intial value ODE solver to solve the well-behaved solutions. This method is numerically stable but difficult to set up, especially when there is more than one exponentially growing mode — for example, in a sixth-order mode conversion equation. Due to these difficulties, all these methods were used to solve a fourth-order mode conversion equation, which has only one exponentially growing mode.

In this paper, we present a finite difference method to solve the mode conversion equation. The method is numerically stable and easy to implement. As can be seen from Sec. 2, the method also gives very accurate solutions compared with analytical asymptotic analysis, whereas the results found by the other methods were not compared with those from asymptotic analysis and their accuracy is hardly known. The main idea of this technique is to first find a set of appropriate boundary conditions which force the exponentially growing modes and other unphysical modes to vanish. Then, these boundary conditions and the mode conversion equations are solved as a standard two-point boundary value problem. In this paper, we will use this method to solve a tunneling equation — one of the mode conversion equations without power absorption. However, the method itself is not limited to this case and can be used to solve any mode conversion equation. For example, a sixth-order mode conversion equation with power absorption and one more exponentially growing mode on each side of the mode conversion layer is discussed in Sec. 4.

The tunneling equation solved in this paper is

$$y^{iv} + \lambda^2 x y'' + (\lambda^2 x + \gamma) y = 0, \tag{1}$$

where $y = y(x)$, $y'' = d^2y/dx^2$, $y^{iv} = d^4y/dx^4$, and λ and γ are constant parameters. The solution for $\gamma < -1$ was analyzed by Faulconer[12]. The solution for $\gamma > -1$ was first analyzed by Erokhin[13], and later by Ngan and Swanson in applying it to the tunneling problem at the ion cyclotron harmonic.[14] The reason we choose this equation as a specific example is that its asymptotic solution for $|x| \to \infty$ is available [14,15] and can be compared with our numerical results. Although Eq. (1) has four independent solutions, in this paper we consider only a fast wave incident from $-\infty$ or $+\infty$, or a slow wave incident from $+\infty$. These solutions are the only three with physical interest, but the other solution can be found in the same fashion.

The organization of this paper is as follows. In Sec. 2 we present the numerical method to solve the tunneling equation (1). In Sec. 3 we give the numerical results and compare our results with those from asymptotic analysis. In Sec. 4 we conclude by discussing the implications of the numerical method.

2 NUMERICAL METHOD

Before we use the finite difference method to solve the tunneling equation as a two-point boundary value problem, we need to find boundary conditions that eliminate the exponentially growing mode and other unphysical modes. We first convert the fourth-order ODE (1) to a set of four first-order ODEs:

$$\frac{d\mathbf{y}}{dx} = \mathbf{M} \cdot \mathbf{y}, \tag{2}$$

where $\mathbf{y} = (y, y', y'', y''')$ and

$$\mathbf{M} = \begin{bmatrix} 0 & 1 & 0 & 0 \\ 0 & 0 & 1 & 0 \\ 0 & 0 & & 1 \\ (\lambda^2 x + \gamma) & 0 & -\lambda^2 x & 0 \end{bmatrix}. \tag{3}$$

The asymptotic solution for large $|x|$ can be expanded in terms of Wentzel-Kramers-Brillouin (WKB) modes. We assume that the WKB mode is

$$\mathbf{y} = \mathbf{Y} \exp\left[i \int^x k(x')\, dx'\right], \tag{4}$$

where $\mathbf{Y}$ is a vector with four elements and has weak dependence on x. Substituting $\mathbf{y}$ into the ODE (2), we obtain a characteristic equation,

$$\det(\mathbf{M} - ik\mathbf{I}) = 0, \tag{5}$$

where $\mathbf{I}$ is the 3×3 unit matrix. The characteristic equation gives four eigenvalues,

$$k = \pm \left\{ \lambda^2 x/2 \pm \left[\lambda^4 x^2/4 - (\lambda^2 x + \gamma)\right]^{1/2} \right\}^{1/2}. \tag{6}$$

Each eigenvalue k has its corresponding eigenvector, $\mathbf{Y} = [1, ik, (ik)^2, (ik)^3]$.

To clearly see the physical meaning of each WKB mode, we expand Eq. (6) for large $|x|$ although the expansion is not needed in our numerical computation. For $x \to -\infty$, we get

$$k^-_{1,2} = \pm 1 \tag{7}$$

and

$$k^-_{3,4} = \mp i\lambda |x|^{1/2}. \tag{8}$$

For $x \to +\infty$, we get

$$k^+_{1,2} = \pm 1 \tag{9}$$

and

$$k^+_{3,4} = \pm \lambda x^{1/2}. \tag{10}$$

The $k = 1$ mode is a fast wave traveling in the $+x$ direction, and the $k = -1$ mode is a fast wave traveling in the $-x$ direction. The k_3^- mode exponentially decays away from the mode conversion layer, and the k_4^- mode exponentially grows, which is the reason for the instability of other numerical techniques. For a physical solution, the growing mode has to be avoided for large $-x$. The k_3^+ mode represents a slow wave having positive phase velocity but negative energy flow.[15] The k_4^+ represents a slow wave having negative phase velocity but positive energy flow.

2.1 Fast wave incident from $-\infty$

For a fast wave incident from $-\infty$ k_1^-, we have a reflected fast wave k_2^- and an exponentially decaying mode k_3^- for $x \to -\infty$. For $x \to +\infty$, we have a transmitted fast wave k_1^+ and a slow wave k_4^+.

The asymptotic solution for $x \to -\infty$ can be expanded as

$$\mathbf{y} = \sum_{i=1}^{4} C_i^- \mathbf{Y}_i^-, \tag{11}$$

where $\mathbf{Y}_i^-$ are the eigenvectors corresponding to eigenvalues k_i^- and the exponential factors $\exp(i \int^x k_i^- \, dx')$ are absorbed into the unknown expansion coefficients C_i^-.

To eliminate the exponentially growing mode k_4^-, we simply set $C_4^- = 0$. In order for Eq. (11) to have nontrivial C_1^-, C_2^-, and C_3^-, we obtain from Eq. (11)

$$\det \begin{bmatrix} y & 1 & 1 & 1 \\ y' & ik_1^- & ik_2^- & ik_3^- \\ y'' & (ik_1^-)^2 & (ik_2^-)^2 & (ik_3^-)^2 \\ y''' & (ik_1^-)^3 & (ik_2^-)^3 & (ik_3^-)^3 \end{bmatrix} = 0, \tag{12}$$

which is a homogenous equation. The physical meaning of this condition is that the exponentially growing mode vanishes at the surface where the condition is imposed. If we can numerically satisfy the above condition, the exponentially growing mode will be avoided.

The asymptotic solution for $x \to +\infty$ can be expanded as

$$\mathbf{y} = \sum_{i=1}^{4} C_i^+ \mathbf{Y}_i^+, \tag{13}$$

where $\mathbf{Y}_i^+$ are the eigenvectors corresponding to eigenvalues k_i^+. To eliminate the unphysical modes k_2^+ and k_3^+ (which represent a fast wave incident from $+\infty$ and a slow wave with energy flowing from $+\infty$, respectively), we set $C_2^+ = C_3^+ = 0$. In order for Eq. (13) to have nontrivial C_1^+ and C_4^+, we obtain from Eq. (13)

$$\det \begin{bmatrix} y & 1 & 1 \\ y' & ik_1^+ & ik_4^+ \\ y'' & (ik_1^+)^2 & (ik_4^+)^2 \end{bmatrix} = 0 \tag{14}$$

and

$$\det \begin{bmatrix} y' & ik_1^+ & ik_4^+ \\ y'' & (ik_1^+)^2 & (ik_4^+)^2 \\ y''' & (ik_1^+)^3 & (ik_4^+)^3 \end{bmatrix} = 0. \tag{15}$$

The physical meaning of these two conditions is that there is no fast wave incident from $+\infty$ or no slow wave energy flowing from $+\infty$.

We solve the set of first-order ODEs (2) with the boundary conditions given by Eq. (12) at $x = x^-$, and Eqs. (14) and (15) at $x = x^+$. A normalization $y = 1$ is used at either end. This is a well-posed two-point boundary value problem: four first-order ODEs and four boundary conditions. Here, x^- and x^+ are chosen far enough from the mode conversion layer so that the asymptotic WKB expansion is valid. In our actual calculation, the eigenvalues are calculated from Eq. (6), rather than Eqs. (7)–(10), and each mode is numerically identified.

2.2 Fast wave incident from $+\infty$

For a fast wave incident from $+\infty$ k_2^+, we have a reflected fast wave k_1^+ and a slow wave k_4^+ for $x \to +\infty$. (Actually, there is no reflected fast wave, but this fact is known only after the ODEs are solved. This fact will serve a good test for the accuracy of the numerical method.) For $x \to -\infty$, we have a transmitted fast wave k_2^- and an exponentially decaying mode k_3^-. To eliminate the fast wave k_1^- incident from $-\infty$ and and the exponentially growing mode k_4^- for $x \to -\infty$, we set $C_1^- = C_4^- = 0$ in Eq. (11) and obtain

$$\det \begin{bmatrix} y & 1 & 1 \\ y' & ik_2^- & ik_3^- \\ y'' & (ik_2^-)^2 & (ik_3^-)^2 \end{bmatrix} = 0 \tag{16}$$

and

$$\det \begin{bmatrix} y' & ik_2^- & ik_3^- \\ y'' & (ik_2^-)^2 & (ik_3^-)^2 \\ y''' & (ik_2^-)^3 & (ik_3^-)^3 \end{bmatrix} = 0. \tag{17}$$

To eliminate the slow wave with energy flowing from $+\infty$, we set $C_3^+ = 0$ in Eq. (13) and have

$$\det \begin{bmatrix} y & 1 & 1 & 1 \\ y' & ik_1^+ & ik_2^+ & ik_4^+ \\ y'' & (ik_1^+)^2 & (ik_2^+)^2 & (ik_4^+)^2 \\ y''' & (ik_1^+)^3 & (ik_2^+)^3 & (ik_4^+)^3 \end{bmatrix} = 0. \tag{18}$$

Equations (16) and (17) at $x = x^-$, Eq. (18) at $x = x^+$, and a normalization $y = 1$ at either end constitute the boundary conditions for a fast wave incident from $+\infty$.

2.3 Slow wave incident from $+\infty$

For a slow wave incident from $+\infty$ k_3^+, we have a fast wave k_1^+ from the mode conversion and a reflected slow wave k_4^+ for $x \to +\infty$. For $x \to -\infty$ we have a fast wave k_2^- from the mode conversion and an exponentially decaying mode k_3^-. To eliminate the fast wave k_1^- incident from $-\infty$ and and the exponentially growing mode k_4^- for $x \to -\infty$, we set $C_1^- = C_4^- = 0$ in Eq. (11) and obtain

$$\det \begin{bmatrix} y & 1 & 1 \\ y' & ik_2^- & ik_3^- \\ y'' & (ik_2^-)^2 & (ik_3^-)^2 \end{bmatrix} = 0 \tag{19}$$

and

$$\det \begin{bmatrix} y' & ik_2^- & ik_3^- \\ y'' & (ik_2^-)^2 & (ik_3^-)^2 \\ y''' & (ik_2^-)^3 & (ik_3^-)^3 \end{bmatrix} = 0. \tag{20}$$

To eliminate the fast wave incident from $+\infty$ for $x \to +\infty$, we set $C_2^+ = 0$ in Eq. (13) and have

$$\det \begin{bmatrix} y & 1 & 1 & 1 \\ y' & ik_1^+ & ik_3^+ & ik_4^+ \\ y'' & (ik_1^+)^2 & (ik_3^+)^2 & (ik_4^+)^2 \\ y''' & (ik_1^+)^3 & (ik_3^+)^3 & (ik_4^+)^3 \end{bmatrix} = 0. \tag{21}$$

Equations (19) and (20) at $x = x^-$, Eq. (21) at $x = x^+$, and a normalization $y = 1$ at either end constitute the boundary conditions for a slow wave incident from $+\infty$.

3 NUMERICAL SOLUTION

Since this is a standard two-point value problem, we use a routine in the Numerical Algorithm Group (NAG) library, which solves a linear two-point boundary value problem for a system of ODEs using a deferred correction technique. Figure 1 shows the dispersion curves found from Eq. (6) for $\lambda = 3$ and $\gamma = 1$. The mode conversion layer is located around $x = 0$.

3.1 Fast wave incident from $-\infty$

Figure 2 shows the numerical solution with boundary conditions given by Eq. (12) imposed at $x = -10$, and by Eqs.(14) and (15) with $y = 1$ at $x = 10$. Since our solution satisfies Eqs. (12), (14) and (15), it does not contain the exponentially growing mode at large $-x$, the incident fast wave from $+\infty$, or the slow wave with energy flowing from $+\infty$.

To check the accuracy of the numerical solution, we calculate a conserved quantity for the tunneling equation (1) [15],

$$P(\mathrm{y}) = y'''y'''^* + y'''y^* - y''y'^* - \gamma y'y^* - c.c. \,. \tag{22}$$

This conserved quantity is related to energy flux in rf heating of plasmas[15] and will be used later to define scattering coefficients. The largest relative error of P for the solution within $(-10, 10)$ shown in Fig. 2 is 3×10^{-6}.

To compare these results with the results from asymptotic analysis, we use the conserved quantity to define the transmission, reflection, and mode conversion coefficients. For a fast wave incident from $-\infty$ towards $+\infty$, we define the transmission coefficient as

$$T_p = \left| \frac{P(C_1^+ \mathbf{Y}_1^+)}{P(C_1^- \mathbf{Y}_1^-)} \right|^2 , \tag{23}$$

the reflection coefficient as

$$R_p = \left| \frac{P(C_2^- \mathbf{Y}_1^-)}{P(C_1^- \mathbf{Y}_1^-)} \right|^2 , \tag{24}$$

and the mode conversion coefficient as

$$C_p = \left| \frac{P(C_4^+ \mathbf{Y}_4^+)}{P(C_1^- \mathbf{Y}_1^-)} \right|^2 , \tag{25}$$

where C_i^- and C_i^+ are defined in Eqs. (11) and (13), respectively, and can be found after the ODEs are solved. Using the asymptotic solutions in Ref. [15], we find that our definitions of T_p, R_p, and C_p are related to T, R and C in Ref. [15] by $T_p = T^2$, $R_p = R^2$, and $C_p = \rho C^2$, where $\rho = (1 - e^{-2\eta})^{-1}$ and $\eta = \pi(1+\gamma)/2\lambda^2$ is called the tunneling factor. Our definitions have the advantage of being independent of the specific WKB mode normalization and are easy to implement in the numerical computation for solutions in a finite domain. Equation (22) implies[15]

$$T_p + R_p + C_p = 1. \tag{26}$$

For the solution shown in Fig. 2, we have $T_p = 49.74\%$, $R_p = 25.22\%$, and $C_p = 25.04\%$. As another check of the numerical accuracy, the sum of T_p, R_p, and C_p differs from unity by 2×10^{-6}. From the asymptotic analysis in Ref. [15], $T_p = e^{-2\eta} = 49.75\%$, $R_p = (1 - e^{-2\eta})^2 = 25.25\%$, and $C_p = e^{-2\eta}(1 - e^{-2\eta}) = 25.00\%$. We can see that our numerical results agree with those from the asymptotic analysis very well.

3.2 Fast wave incident from $+\infty$

For a fast wave incident from $+\infty$, we solve the ODEs given by Eq. (2) with boundary conditions given by Eqs. (16) and (17) at $x = -10$, and by Eq. (18) and $y = 1$ at $x = 10$. The solution is shown in Fig. 3. The largest relative error of the conserved quantity P defined in Eq. (22) is 8×10^{-6}. Now the transmission, the reflection, and the mode conversion coefficients are defined as

$$T_p = \left| \frac{P(C_2^- \mathbf{Y}_2^-)}{P(C_2^+ \mathbf{Y}_2^+)} \right|^2 , \tag{27}$$

$$R_p = \left| \frac{P(C_1^+ \mathbf{Y}_1^+)}{P(C_2^+ \mathbf{Y}_2^+)} \right|^2 , \tag{28}$$

$$C_p = \left| \frac{P(C_4^+ \mathbf{Y}_4^+)}{P(C_2^+ \mathbf{Y}_2^+)} \right|^2 . \tag{29}$$

The numerical results of these coefficients for the solution shown in Fig. 3 are $T_p = 49.74\%$, $R_p = 1.2 \times 10^{-6}$, and $C_p = 50.26\%$. The sum of T_p, R_p, and C_p differs from unity by 4×10^{-6}. From the asymptotic analysis in Ref. [15], $T_p = e^{-2\eta} = 49.75\%$, $R_p = 0$, and $C_p = 1 - e^{-2\eta} = 50.25\%$. Note that the boundary condition given by Eq. (18) allows the presence of the reflected fast wave, but, as expected from asymptotic analysis[15], the solution of the ODEs does not contain the reflected fast wave. This provides another demonstration of the accuracy of the numerical method.

3.3 Slow wave incident from $+\infty$

For a slow wave incident from $+\infty$, we solve the ODEs given by Eq. (2) with Eqs. (19) and (20) for boundary conditions at $x = -10$. Equation (21) and $y = 1$ are used for boundary conditions at $x = 10$. The solution is shown in Fig. 4. The largest relative error of the conserved quantity P defined in Eq. (22) is 2.3×10^{-5}. The coefficients for the mode conversion to a fast wave traveling towards $-\infty$, the slow wave reflection, and the mode conversion to a fast wave traveling towards $+\infty$ are defined as

$$C_p^- = \left| \frac{P(C_2^- \mathbf{Y}_2^-)}{P(C_3^+ \mathbf{Y}_3^+)} \right|^2 , \tag{30}$$

$$R_p = \left| \frac{P(C_4^+ \mathbf{Y}_4^+)}{P(C_3^+ \mathbf{Y}_3^+)} \right|^2 , \tag{31}$$

$$C_p^+ = \left| \frac{P(C_1^+ \mathbf{Y}_1^+)}{P(C_3^+ \mathbf{Y}_3^+)} \right|^2 . \tag{32}$$

The numerical results of these coefficients for the solution shown in Fig. 4 are $C_p^+ = 25.04\%$, $R_p = 24.70\%$, and $C_p^- = 50.26\%$. The sum of C_p^-, R_p, and C_p^+ differs from unity by 6×10^{-6}. The solution from the asymptotic analysis in Ref. [15] is $C_p^- = e^{-2\eta}(1 - e^{-2\eta}) = 25.00\%$, $R_p = e^{-4\eta} = 24.75\%$, and $C_p^+ = 1 - e^{-2\eta} = 50.25\%$.

4 CONCLUSION

In this paper we demonstrate that a finite difference method can be used to solve a mode conversion equation without the difficulty of exponentially growing modes associated with other techniques. This numerical method is quite general and can be applied to solve any mode conversion equation provided appropriate boundary conditions can be found to eliminate unphysical components of the solutions. The ODEs can then be easily solved by using a standard two-point boundary value solver. This technique has also been successfully applied to solve a sixth-order mode conversion equation with power absorption. The sixth-order equation has one more exponentially growing mode on each side of the mode conversion layer compared with the fourth-order tunneling equation (1). These results will be reported in a future publication.

ACKNOWLEDGMENTS

The work of C. Y. Wang is supported by an appointment to the Oak Ridge National Laboratory Postdoctoral Research Associates Program, administrated jointly by the Oak Ridge Institute for Science and Education and the Oak Ridge National Laboratory. The work of M. D. Carter, D. B. Batchelor, and E. F. Jaeger is supported by the U.S. Department of Energy under Contract No. DE-AC05-84OR21400 with Martin Marietta Energy Systems, Inc.

REFERENCES

[1] FUKUYAMA, A., K. ITOH, and S.-I. ITOH, Comput. Phys. Rep. **4** (1986) 137.

[2] SHOKAIR, I. R., R. W. CONN, and T. K. MAU, Nucl. Fusion **28** (1988) 1393.

[3] JAEGER, E. F., D. B. BATCHELOR, and H. WEITZNER, Nucl. Fusion **28** (1988) 53.

[4] BRAMBILLA, M., Nucl. Fusion **28** (1988) 549.

[5] SWANSON, D. G., Phys. Fluids **21** (1978) 926.

[6] CHIU, S. C., and T. K. MAU, Nucl. Fusion **23** (1983) 1613.

[7] COLSETOCK, P. L., and R. J. KASHUBA, Nucl. Fusion **23** (1983) 763.

[8] ROMERO, H., and J. SCHARER, Nucl. Fusion **27** (1987) 363.

[9] SUND, R. S., and J. E. SCHARER, Phys. Fluids B **3** (1991) 1326.

[10] SWANSON, D. G., Phys. Fluids **28** (1985) 2645.

[11] STIX, T. H., and D. G. SWANSON, in *Handbook of Plasma Physics*, edited by A. GALEEV and R. N. SUDAN (North Holland, Amsterdam, 1983), Vol. 1, p. 335.

[12] FAULCONER, D. W., Phys. Lett. **75A** (1980) 355.

[13] EROKHIN, N. S., Ukr. Fiz. Zh. **14** (1969) 2055.

[14] NGAN, Y. C., and D. G. SWANSON, Phys. Fluids **20** (1977) 1920.

[15] SWANSON, D. G., *Plasma Waves* (Academic Press, New York, 1989).

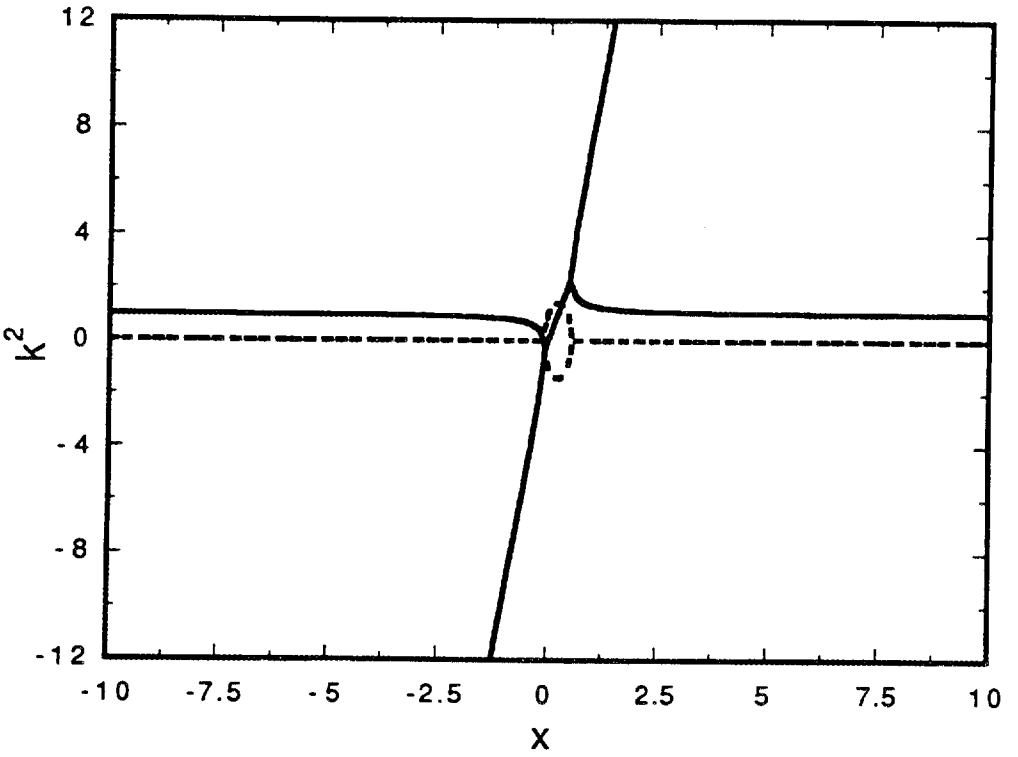

Figure 1: The dispersion curves for the tunneling equation (1) with $\lambda = 3$ and $\gamma = 1$. The solid and dashed lines represent the real and imaginary parts, respectively, of k^2.

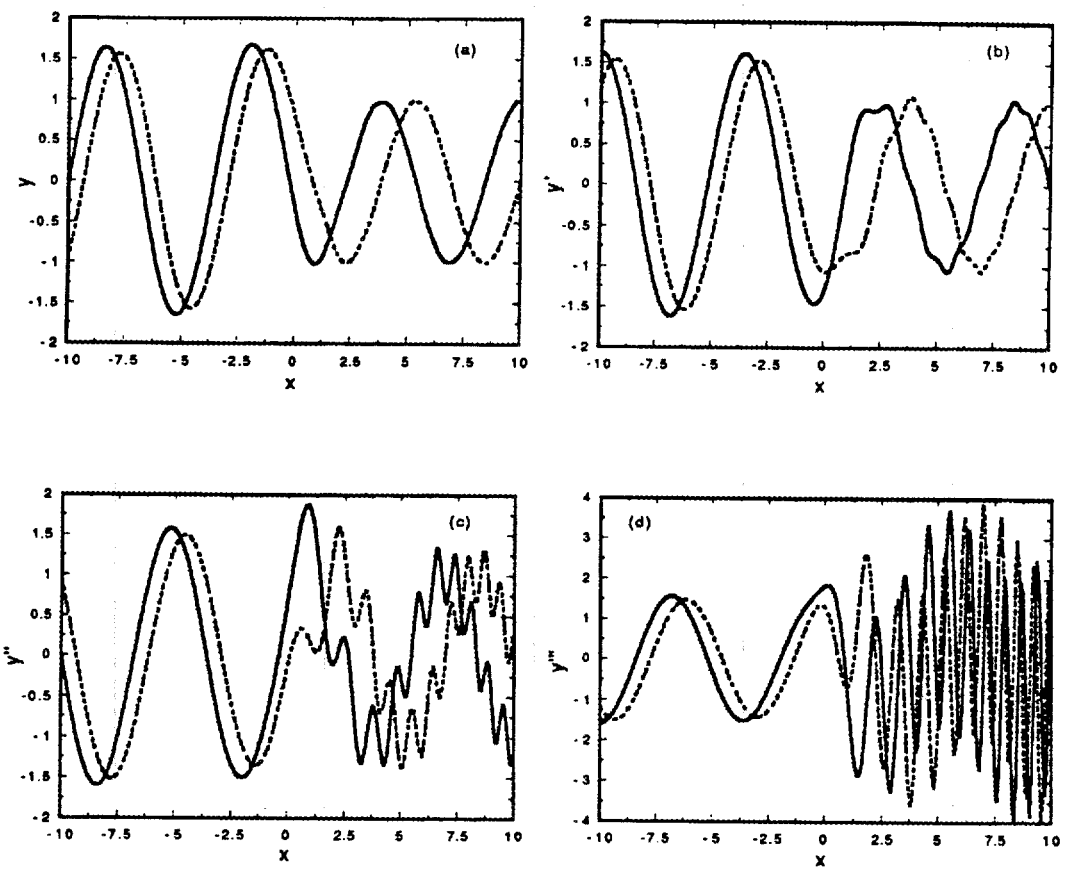

Figure 2: The numerical solution for the tunneling equation (1) with $\lambda = 3$ and $\gamma = 1$, and a fast wave incident from $-\infty$: (a) y vs x, (b) y' vs x, (c) y'' vs x, and (d) y''' vs x. The solid lines are real parts, and the dotted lines are imaginary parts.

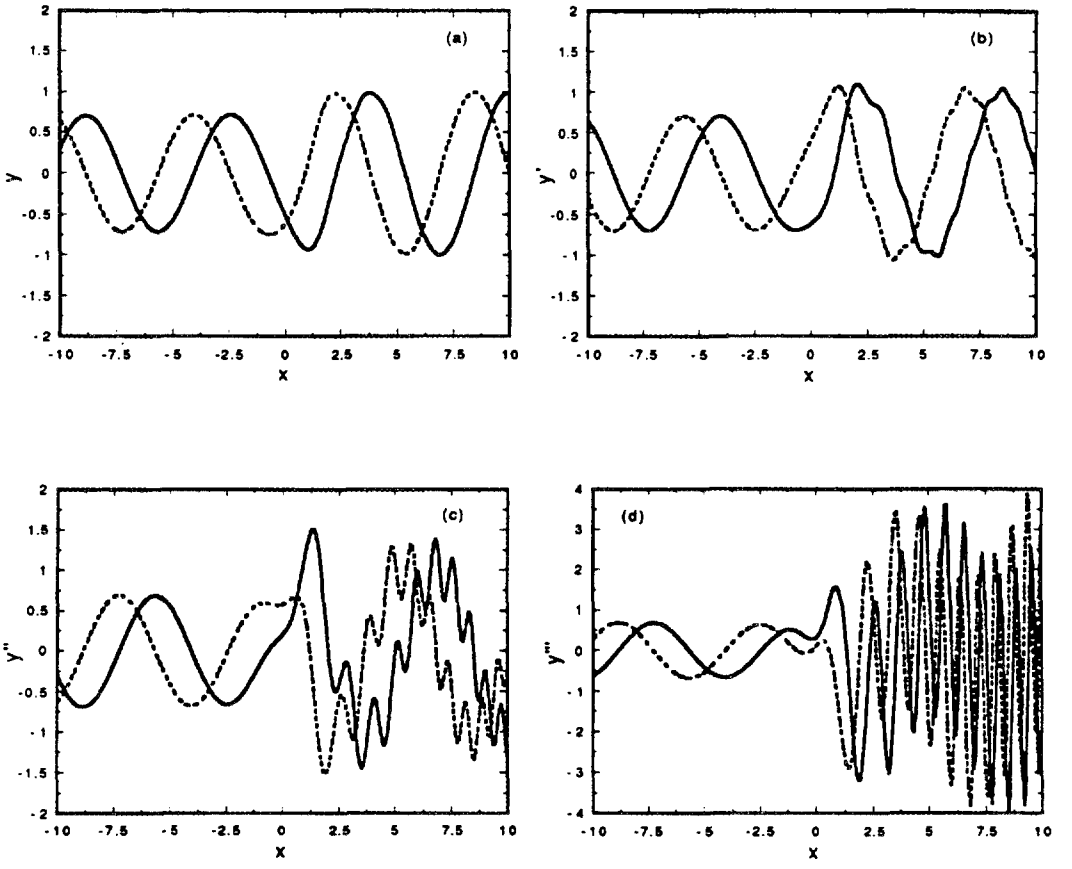

Figure 3: The numerical solution for the tunneling equation (1) with $\lambda = 3$ and $\gamma = 1$, and a fast wave incident from $+\infty$: (a) y vs x, (b) y' vs x, (c) y'' vs x, and (d) y''' vs x. The solid lines are real parts and the dotted lines are imaginary parts.

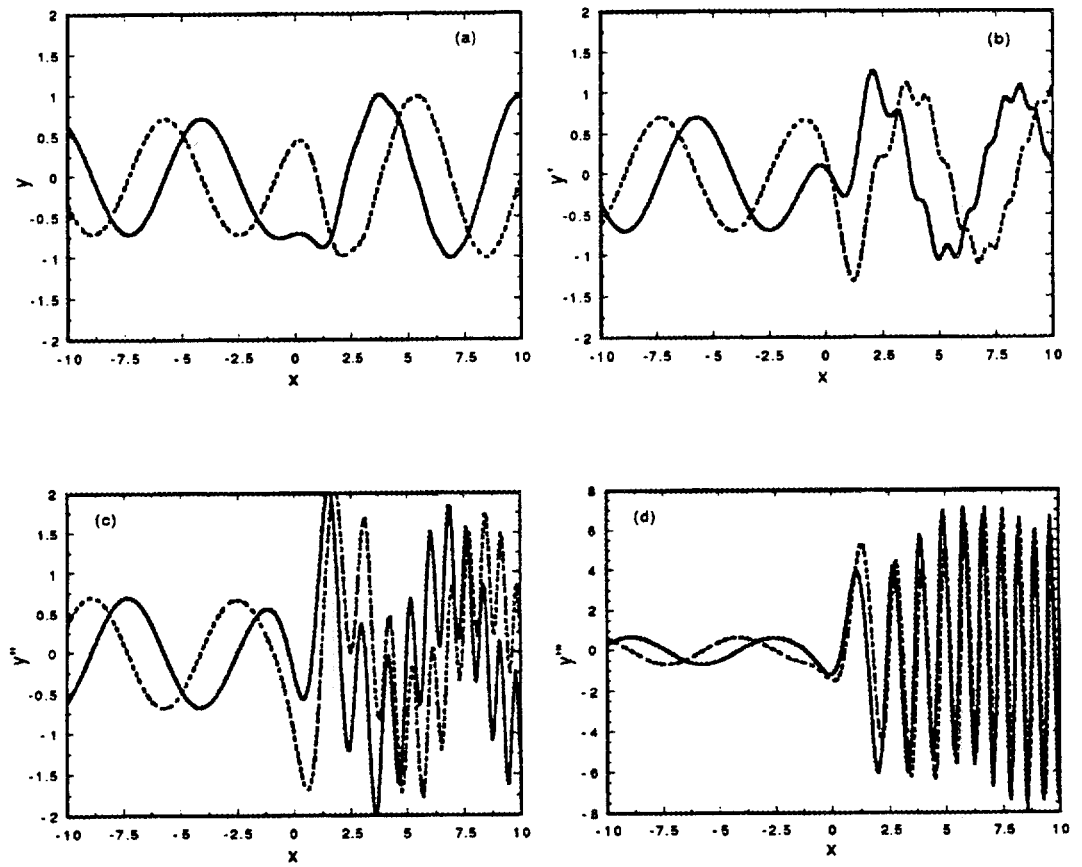

Figure 4: The numerical solution for the tunneling equation (1) with $\lambda = 3$ and $\gamma = 1$, and a slow wave incident from $+\infty$: (a) y vs x, (b) y' vs x, (c) y'' vs x, and (d) y''' vs x. The solid lines are real parts and the dotted lines are imaginary parts.

INTERNAL DISTRIBUTION

1. Director, ORNL Fusion Energy Division
2. C. C. Baker
3. L. A. Berry
4. B. A. Carreras
5. H. E. Clark
6. R. I. Colchin
7. R. A. Dory
8. J. L. Dunlap
9. F. E. Gethers
10. T. E. Shannon
11. W. L. Stirling

12–13. Laboratory Records Department
14. Laboratory Records, ORNL-RC
15–16. Central Research Library
17. Document Reference Section
18. Fusion Energy Division Library
19–20. ET/FE Division Publications Office
21. ORNL Patent Office
22–26. D. B. Batchelor
27. M. D. Carter
28. F. W. Baity
29. T. S. Bigelow
30. R. C. Goldfinger
31. R. H. Goulding
32. S. P. Hirshman
33. D. J. Hoffman
34. W. A. Houlberg
35. E. F. Jaeger
36. S. L. Milora
37. D. A. Rasmussen
38. P. M. Ryan
39. D. C. Stallings
40. D. W. Swain
41-45. C. Y. Wang
46. J. H. Whealton
47. J. J. Yugo

EXTERNAL DISTRIBUTION

48. Office of the Assistant Manager for Energy Research and Development, Department of Energy, Oak Ridge Operations, P.O. Box 2000, Oak Ridge, TN 37831
49. N. A. Davies, Director, Office of Fusion Energy, Office of Energy Research, ER-50 Germantown, U.S. Department of Energy, Washington, DC 20545
50. M. Roberts, International Programs, Office of Fusion Energy, Office of Energy Research, ER-52 Germantown, U.S. Department of Energy, Washington, DC 20545
51. D. E. Baldwin, Lawrence Livermore National Laboratory, P.O. Box 5511, Livermore, CA 94550
52. R. W. Conn, Mechanical, Aerospace, and Nuclear Engineering Department, 6291 Boelter Hall, University of California, Los Angeles, CA 90024-1597
53. P. C. Liewer, MS 138-208, Jet Propulsion Laboratory, 4800 Oak Grove Drive, Pasadena, CA 91109
54. D. Sigmar, Plasma Fusion Center, Massachusetts Institute of Technology, 167 Albany St., NW16-288, Cambridge, MA 02139
55. K. I. Thomassen, L-637, Lawrence Livermore National Laboratory, P.O. Box 5511, Livermore, CA 94550
56. J. D. Callen, Department of Nuclear Engineering, University of Wisconsin, Madison, WI 53706-1687
57. S. O. Dean, Fusion Power Associates, Inc., 2 Professional Drive, Suite 248, Gaithersburg, MD 20879
58. H. K. Forsen, Bechtel Group, Inc., Research Engineering, P.O. Box 3965, San Francisco, CA 94119

59. R. W. Gould, Department of Applied Physics, California Institute of Technology, Pasadena, CA 91125
60. R. A. Gross, Plasma Research Laboratory, Columbia University, New York, NY 10027
61. R. J. Hawryluk, Plasma Physics Laboratory, Princeton University, P.O. Box 451, Princeton, NJ 08543
62. D. M. Meade, Plasma Physics Laboratory, Princeton University, P.O. Box 451, Princeton, NJ 08543
63. W. M. Stacey, School of Nuclear Engineering and Health Physics, Georgia Institute of Technology, Atlanta, GA 30332
64. D. Steiner, Nuclear Engineering Department, NES Building, Tibbetts Avenue, Rensselaer Polytechnic Institute, Troy, NY 12181
65. R. Varma, Physical Research Laboratory, Navrangpura, Ahmedabad 380009, India
66. Bibliothek, Max-Planck Institut für Plasmaphysik, Boltzmannstrasse 2, D-8046 Garching, Federal Republic of Germany
67. Bibliothek, Institut für Plasmaphysik, KFA Jülich GmbH, Postfach 1913, D-5170 Jülich, Federal Republic of Germany
68. Bibliothek, KfK Karlsruhe GmbH, Postfach 3640, D-7500 Karlsruhe 1, Federal Republic of Germany
69. Bibliotheque, Centre de Recherches en Physique des Plasmas, Ecole Polytechnique Fédérale de Lausanne, 21 Avenue des Bains, CH-1007 Lausanne, Switzerland
70. R. Aymar, CEN/Cadarache, Departement de Recherches sur la Fusion Contrôlée, F-13108 Saint-Paul-lez-Durance Cedex, France
71. Bibliothèque, CEN/Cadarache, F-13108 Saint-Paul-lez-Durance Cedex, France
72. Library, JET Joint Undertaking, Abingdon, Oxfordshire OX14 3EA, England
73. Library, FOM-Instituut voor Plasmafysica, Rijnhuizen, Edisonbaan 14, 3439 MN Nieuwegein, The Netherlands
74. Library, National Institute for Fusion Science, Chikusa-ku, Nagoya 464-01, Japan
75. Library, International Centre for Theoretical Physics, P.O. Box 586, I-34100 Trieste, Italy
76. Library, Centro Richerche Energia Frascati, C.P. 65, I-00044 Frascati (Roma), Italy
77. Library, Plasma Physics Laboratory, Kyoto University, Gokasho, Uji, Kyoto 611, Japan
78. Plasma Research Laboratory, Australian National University, P.O. Box 4, Canberra, A.C.T. 2601, Australia
79. Library, Japan Atomic Energy Research Institute, Naka Fusion Research Establishment, 801-1 Mukoyama, Naka-machi, Naka-gun, Ibaraki-ken, Japan
80. G. A. Eliseev, I. V. Kurchatov Institute of Atomic Energy, P.O. Box 3402, 123182 Moscow, Russia
81. V. A. Glukhikh, Scientific-Research Institute of Electro-Physical Apparatus, 188631 St. Petersburg, Russia
82. I. Shpigel, Institute of General Physics, U.S.S.R. Academy of Sciences, Ulitsa Vavilova 38, Moscow, Russia
83. D. D. Ryutov, Institute of Nuclear Physics, Siberian Academy of Sciences, Sovetskaya St. 5, 630090 Novosibirsk, Russia
84. O. Pavlichenko, Kharkov Physical-Technical Institute, Academical St. 1, 310108 Kharkov, Ukraine
85. Deputy Director, Southwestern Institute of Physics, P.O. Box 15, Leshan, Sichuan, China (PRC)
86. Director, The Institute of Plasma Physics, P.O. Box 1126, Hefei, Anhui, China (PRC)
87. R. H. McKnight, Experimental Plasma Research Branch, Division of Development and Technology, Office of Fusion Energy, Office of Energy Research, ER-542 Germantown, U.S. Department of Energy, Washington, DC 20545
88. D. Crandall, Director, Division of Applied Plasma Physics, Office of Fusion Energy, Office of Energy Research, ER-54 Germantown, U.S. Department of Energy, Washington, DC 20545

89. E. Oktay, Division of Confinement Systems, Office of Fusion Energy, Office of Energy Research, ER-55 Germantown, U.S. Department of Energy, Washington, DC 20545
90. W. Sadowski, Fusion Theory and Computer Services Branch, Division of Applied Plasma Physics, Office of Fusion Energy, Office of Energy Research, ER-541 Germantown, U.S. Department of Energy, Washington, DC 20545
91. R. E. Mickens, Atlanta University, Department of Physics, Atlanta, GA 30314
92. M. N. Rosenbluth, University of California at San Diego, La Jolla, CA 92037
93. D. Schnack, SAIC, 10260 Campus Point Drive, San Diego, CA 92121
94. Duk-In Choi, Department of Physics, Korea Advanced Institute of Science and Technology, P.O. Box 150, Chong Ryang-Ri, Seoul, Korea
95. Library of Physics Department, University of Ioannina, Ioannina, Greece
96. C. De Palo, Library, Associazione EURATOM-ENEA sulla Fusione, CP 65, I-00044 Frascati (Roma), Italy
97. Laboratorio Associado de Plasma, Instituto Nacional de Pesquisas Espaciais, Caixa Postal 515, 122201, Sao Jose dos Campos, SP, Brazil
98. Theory Department Read File, c/o D. W. Ross, University of Texas, Institute for Fusion Studies, Austin, TX 78712
99. Theory Department Read File, c/o R. Parker, Director, Plasma Fusion Center, NW 16-202, Massachusetts Institute of Technology, Cambridge, MA 02139
100. Theory Department Read File, c/o R. White, Plasma Physics Laboratory, Princeton University, P.O. Box 451, Princeton, NJ 08543
101. Theory Department Read File, c/o L. Kovrizhnykh, Lebedev Institute of Physics, Academy of Sciences, 53 Leninsky Prospect, 117924 Moscow, Russia
102. Theory Department Read File, c/o B. B. Kadomtsev, I. V. Kurchatov Institute of Atomic Energy, P.O. Box 3402, 123182 Moscow, Russia
103. Theory Department Read File, c/o T. Kamimura, National Institute for Fusion Studies, Nagoya 464, Japan
104. Theory Department Read File, c/o E. Maschke, Departemente de Recherches sur la Fusion Controlée, CEN/Cadarache, F-13108 Saint-Paul-lez Durance, France
105. Theory Department Read File, c/o D. Düchs, JET Joint Undertaking, Abingdon, Oxfordshire OX14 3EA, United Kingdom
106. Theory Department Read File, c/o R. Briscoe, Culham Laboratory, Abingdon, Oxfordshire OX14 3DB, United Kingdom
107. Theory Department Read File, c/o D. Biskamp, Max-Planck-Institut fur Plasmaphysik, Boltzmannstrasse 2, D-8046 Garching, Federal Republic of Germany
108. Theory Department Read File, c/o T. Takeda, Japan Atomic Energy Research Institute, Tokai Fusion Research Establishment, Tokai-mura, Naka-gun, Ibaraki-ken, Japan
109. Theory Department Read File, c/o J. Greene, General Atomics, P.O. Box 85608, San Diego, CA 92186
110. Theory Department Read File, c/o R. Cohen, Lawrence Livermore National Laboratory, P.O. Box 5511, Livermore, CA 94550
111. Theory Department Read File, c/o R. Gerwin, CTR Division, Los Alamos National Laboratory, P.O. Box 1663, Los Alamos, NM 87545
112. R. Aamodt, Lodestar Research Corporation, 2400 Central Avenue, Boulder, CO 80301
113. K. Appert, Centre de Recherches en Physique des Plasmas, Ecole Polytechnique Fédérale de Lausanne, 21 Avenue des Bains, CH-1007 Lausanne, Switzerland
114. M. Ballico, Max-Planck Institut für Plasmaphysik, Boltzmannstrasse 2, D-8046 Garching, Federal Republic of Germany
115. E. Barbato, Associazione EURATOM–ENEA sulla Fusione, Centro Richerche Energia Frascati, C.P. 65, I-00044 Frascati (Roma), Italy
116. A. Bécoulet, Association EURATOM-CEA sur la Fusion Controlée, Centre d'Etudes Nucléaires de Cadarache, B. P. No. 1, F-13108 Saint Paul lez Durances, France

117. S. Bernabei, Plasma Physics Laboratory, Princeton University, P.O. Box 451, Princeton, NJ 08543
118. A. Bers, Plasma Fusion Center, Massachusetts Institute of Technology, 38-260, Cambridge, MA 02139
119. V. Bhatnagar, JET Joint Undertaking, Abingdon, Oxfordshire OX14 3EA, England
120. P. T. Bonoli, Plasma Fusion Center, Massachusetts Institute of Technology, 175 Albany St., NW17-115, Cambridge, MA 02139
121. M. Brambilla, Max-Planck Institut für Plasmaphysik, Boltzmannstrasse 2, D-8046 Garching, Federal Republic of Germany
122. Dr. Vincent Chan, General Atomics, P. O. Box 85608, San Diego, CA 92186
123. D. Ehst, Building 205, Argonne National Laboratory, 9700 S. Cass Avenue, Argonne, IL 60538
124. D. Faulconer, Laboratoire de Physique des Plasmas, EURATOM–Etat Belge, Ecole Royale Militaire, Avenue de la Renaissance 30, 1040 Brussels, Belgium
125. D. J. Gambier, JET Joint Undertaking, Abingdon, Oxfordshire OX14 3EA, England
126. S. N. Golovato, Plasma Fusion Center, Massachusetts Institute of Technology, 175 Albany Street, NW17-113, Cambridge, MA 02139
127. W. Ho, SAIC, 10260 Campus Point Drive, San Diego, CA 92121
128. J. Hosea, Plasma Physics Laboratory, Princeton University, P.O. Box 451, Princeton, NJ 08543
129. Kwok Ko, Stanford Linear Accelerator Center, P.O. Box 4349, Stanford, CA 94309
130. C. C. Petty, General Atomics, P.O. Box 85608, San Diego, CA 92186
131. C. K. Phillips, Plasma Physics Laboratory, Princeton University, P.O. Box 451, Princeton, NJ 08543
132. M. Porkolab, Plasma Fusion Center, Massachusetts Institute of Technology, 175 Albany Street, NW17-119, Cambridge, MA 02139
133. R. Prater, General Atomics, P.O. Box 85608, San Diego, CA 92186
134. J. Scharer, Electrical and Computer Engineering Department, 1500 Johnson Drive, University of Wisconsin, Madison, WI 53706
135. P. E. Vandenplas, Laboratoire de Physique des Plasmas, EURATOM–Etat Belge, Ecole Royale Militaire, Avenue de la Renaissance 30, 1040 Brussels, Belgium
136. H. Weitzner, Courant Institute for Mathematical Sciences, New York University, 251 Mercer Street, New York, NY 10001
137. J. R. Wilson, Plasma Physics Laboratory, Princeton University, P.O. Box 451, Princeton, NJ 08543

138–185. Given distribution according to OSTI-4500, Magnetic Fusion Energy (Category Distribution UC-427, Theoretical Plasma Physics)